

SYNERGY OF STOCHASTIC AND SYSTEMATIC ENERGIZATION OF PLASMAS DURING TURBULENT RECONNECTION

THEOPHILOS PISOKAS, LOUKAS VLAHOS AND HEINZ ISLIKER

Department of Physics, Aristotle University of Thessaloniki
GR-52124 Thessaloniki, Greece

(Dated: October 10, 2018)

ABSTRACT

The important characteristic of turbulent reconnection is that it combines large scale magnetic disturbances ($\delta B/B \sim 1$) with randomly distributed Unstable Current Sheets (UCSs). Many well known non linear MHD structures (strong turbulence, current sheet(s), shock(s)) lead asymptotically to the state of turbulent reconnection. We analyze in this article, for the first time, the energization of electrons and ions in a **large scale** environment that **combines** large amplitude disturbances propagating with sub-Alfvénic speed with UCSs. The magnetic disturbances interact stochastically (second order Fermi) with the charged particles and they play a crucial role in the heating of the particles, while the UCS interact systematically (first order Fermi) and play a crucial role in the formation of the high energy tail. The synergy of stochastic and systematic acceleration provided by the mixture of magnetic disturbances and UCSs influences the energetics of the thermal and non-thermal particles, the power law index, and the time the particles remain inside the energy release volume. We show that this synergy can explain the observed very fast and impulsive particle acceleration and the slightly delayed formation of a super-hot particle population.

Keywords: particle acceleration, turbulence, Sun:flares, magnetic reconnection

1. INTRODUCTION

Turbulent reconnection can be generated by different, well known, non-linear MHD processes and structures, which serve as their driver, e.g. the evolution of a spectrum of large amplitude MHD waves, the fragmentation of a current sheet(s), or shock(s) (see the reviews of [Matthaeus & Velli 2011](#); [Cargill et al. 2012](#); [Lazarian et al. 2012](#); [Hoshino & Lyubarsky 2012](#); [Karimabadi et al. 2013](#); [Karimabadi et al. 2013](#); [Lazarian et al. 2015](#), and the recent articles of [Zank et al. 2015](#); [Matsumoto et al. 2015](#) on turbulent reconnection driven by shocks, for a brief, yet incomplete, outline of the relevant literature).

The term “turbulent reconnection” appeared first in the article of [Matthaeus & Lamkin \(1986\)](#), and several years later the analytical theory of turbulent reconnection was formulated by [Lazarian & Vishniac \(1999\)](#). In both articles, the role of weak turbulence in the evolution of a reconnecting current sheet was analyzed. In the present article, we expand the term “turbulent reconnection” to denote the co-existence of “large scale coherent magnetic disturbances” ([Kuramitsu & Hada 2000](#); [Greco et al. 2010](#); [Malapaka & Müller 2013](#)) with “unstable current sheets” (UCSs). It has been shown that these two types of nonlinear structures drive and

re-enforce each other ([Karimabadi et al. 2013](#); [Uritsky et al. 2017](#)).

There are at least three avenues that lead to the generation of turbulent reconnection. The first is strong turbulence ([Biskamp & Welter 1989](#); [Dmitruk et al. 2003](#); [Dmitruk et al. 2004](#); [Arzner et al. 2006](#); [Islaker et al. 2017b](#)). The second is the fragmentation of UCSs: numerous studies have explored the evolution of one or multiple UCSs and have shown that they evolve into a turbulent reconnection environment ([Matthaeus & Lamkin 1986](#); [Lazarian & Vishniac 1999](#); [Onofri et al. 2004](#); [Loureiro et al. 2009](#); [Cassak & Drake 2009](#); [Kowal et al. 2011](#); [Hoshino 2012](#); [Uritsky et al. 2017](#)). The third avenue lies downstream of a shock where turbulent reconnection can be driven when the shock is formed in the presence of upstream turbulent flows, e.g. as it is the case with the Earth’s Bow shock and the solar wind, or with coronal mass ejections traveling inside the turbulent solar wind ([Matsumoto et al. 2015](#); [Zank et al. 2015](#); [Burgess et al. 2016](#)).

Several authors explored the formation of turbulent reconnection in the solar atmosphere, driven by the turbulent convection zone ([Parker 1983, 1988](#); [Einaudi & Velli 1994](#); [Galsgaard & Nordlund 1996, 1997a,b](#); [Georgoulis et al. 1998](#); [Rappazzo et al. 2010, 2013](#)). All these

studies focused on the formation of UCSs; large amplitude magnetic disturbances were though also present, yet never analyzed in detail until recently (Kontar et al. 2017).

The solar wind is probably the most striking example of a turbulently reconnecting plasma flow, and the co-existence of large amplitude magnetic disturbances and UCSs has been analyzed in detail by several authors (Greco et al. 2010; Osman et al. 2014; Chasapis et al. 2015).

It is natural to expect that in relativistic jets and other astrophysical flows (e.g. accretion discs) turbulent reconnection will be present, but details have not been worked out yet (Giannios 2010; Sironi et al. 2015; Brunetti & Lazarian 2016). The acceleration mechanism preferred by most researchers as the best candidate for explaining the explosive phenomena in astrophysics remains diffusive shock acceleration, which can be the host of turbulent reconnection (Matsumoto et al. 2015; Zank et al. 2015). The relative importance of the two systematic accelerators (shock acceleration and turbulent reconnection) has not yet been established.

Karimabadi et al. (2013); Uritsky et al. (2017) pointed out that intermittent plasma turbulence will in general consist of both, coherent structures (UCSs) and large amplitude waves (see also Wang et al. 2015; Liang et al. 2016), and the picture given in (Kowal et al. 2017) for the MHD evolution of a single small scale UCS. With their simulations they have presented evidence for the excitation of eddies and waves by the motion of fragmented UCSs. They also noted that this complex environment, which we call here turbulent reconnection, heats very efficiently the plasma.

The evolution of an ensemble of charged particles in turbulent reconnection was investigated by several authors using test particle simulations in snapshots of MHD codes (Ambrosiano et al. 1988; Dmitruk et al. 2004; Turkmani et al. 2005; Arzner et al. 2006; Onofri et al. 2006; Isliker et al. 2017b).

Several authors (Vlahos et al. 2016; Pisokas et al. 2017; Isliker et al. 2017a) analyzed the statistical properties of ions and electrons scattered either off large amplitude magnetic disturbances propagating with the Alfvén speed (Alfvénic Scatterers, ASs), or off UCSs, randomly distributed inside the energy release volume. The interaction of electrons and ions with the accelerators is either stochastic when they interact with Alfvénic disturbances, as in the model proposed initially by Fermi (1949), or systematic, when they interact with UCSs (Fermi 1954). The stochastic energization of ions and electrons leads the initial Maxwellian energy distribution to an asymptotic state and the final distribution is a mixture of a hot and an accelerated plasma, with a power law tail with index ~ 2 . The acceleration time for

parameters related with the solar corona is close to a few seconds (see details in Vlahos et al. 2016; Pisokas et al. 2017). In the case of systematic acceleration, when the energy release volume is dominated by UCSs, the particles are mostly accelerated, forming a power law tail with index ≥ 1 on sub-second time scales, and heating is practically absent (see Vlahos et al. 2016; Isliker et al. 2017a).

In most laboratory and astrophysical plasmas the explosive energy release is associated with intense and efficient heating of the bulk of the plasma and with the formation of a power law tail on very fast time scales (see for example the evolution of the photon distribution for solar flares analyzed by Lin et al. 2003). Lin et al. (2003) pointed out that in the initial rise of a flare substantial particle acceleration is taking place and in the subsequent impulsive phase a coronal super-hot component appears. A possible explanation for the prompt acceleration and the delayed appearance of the super-hot plasma may be related with the differences in the acceleration times between UCSs and the ASs, as reported above. In summary, the synergy of large scale magnetic disturbances and UCSs in turbulent reconnection can provide the explanation for the appearance of impulsive heating of the super-hot sources and of the non-thermal tails.

In this article, we assume that the energy release volume is in the state of turbulent reconnection and the nonlinear structures (magnetic disturbances and UCSs, interchangeably called here “active grid points” or “scatterers”) are randomly distributed. The charged particles scatter off the active grid points and gain or lose energy. The scatterers are divided into two classes, a fraction P ($0 \leq P \leq 1$) are magnetic disturbances (ASs) and the rest ($1 - P$) are UCSs. When $P = 0$ all scatterers are UCS and when $P = 1$ all scatterers are magnetic disturbances (see Vlahos et al. 2016; Pisokas et al. 2017; Isliker et al. 2017a, for studies of the extreme cases).

2. MIXING STOCHASTIC AND SYSTEMATIC SCATTERERS

2.1. *The initial set-up*

The scatterers are randomly chosen and uniformly distributed grid points of a 3D lattice that has linear size L and consists of $(N \times N \times N)$ nodes, with grid size $\ell = L/(N - 1)$. The N_{sc} scatterers form a small fraction $R = N_{sc}/N^3$ of the total number of nodes, and they are either ASs or UCSs, as described above. The mean free path between scatterers can be determined as $\lambda_{sc} = \ell/R$. An ensemble of particles (electrons or ions) are injected into the simulation volume at random grid points, with random direction of motion, and they are allowed to move along the straight lattice edges until

they encounter an active grid point. Encounters with scatterers cause a particle to change its direction of motion and to renew its energy by the amount ΔW , which depends on the physical characteristic of the scatterer. This process repeats up to final time or until a particle reaches the lattice boundary and escapes. (See [Vlahos et al. 2016](#); [Pisokas et al. 2017](#); [Isliker et al. 2017a](#), for a more complete description of the model.)

We assume that the simulation volume has length $L = 10\,000$ km, the active grid points ratio is $R = 5\text{--}15\%$, and the injected particles follow a Maxwellian distribution with temperature $T \approx 1 \cdot 10^6$ K. If a scatterer is an AS, the change in energy of a particle amounts to

$$\frac{\Delta W^{(\text{AS})}}{W} \approx \frac{2}{c^2} (V^2 - \vec{V} \cdot \vec{u}), \quad (1)$$

where for head on collisions $\vec{V} \cdot \vec{u} < 0$ and the particle gains energy, for overtaking collisions $\vec{V} \cdot \vec{u} > 0$ and the particle loses energy ([Pisokas et al. 2017](#)). The ASs, as stochastic scatterers, transfer energy either to or from an interacting particle, but the overall result for the particles is a gain in energy, with a typical increment of the order of $(\Delta W/W) \approx (V_A/c)^2 \sim 5 \cdot 10^{-4}$.

With an UCS as scatterer, the energy gain is caused by the electric field ([Kowal et al. 2011](#); [Isliker et al. 2017a](#)), and it is given by

$$\Delta W^{(\text{EF})} = |q| E_{\text{eff}} \ell_{\text{eff}} \quad (2)$$

where $E_{\text{eff}} \approx (V/c) \delta B$ is a measure of the effective electric field of the UCS, and δB is the fluctuating magnetic field, which is of stochastic nature, as related to the stochastic fluctuations induced by reconnection. The energy increments in eq. (2) are always positive, as it was shown to hold in different particle in cell simulations ([Guo et al. 2015](#); [Dahlin et al. 2015](#); [Matsumoto et al. 2015](#)), and they do not depend on the instantaneous energy of a particle, instead they are proportional to the magnetic field fluctuations δB . The latter are assumed to follow a Kolmogorov spectrum, i.e. they obey a power law distribution with index $5/3$ in the range $[10^{-5} \text{ G}, 100 \text{ G}]$. The effective length ℓ_{eff} of the interaction of a particle with a UCS is assumed an increasing linear function of E_{eff} (so that small E_{eff} are associated with small scale UCS), restricted to values between 10 m and 1 km (see more details in [Isliker et al. 2017a](#)).

2.2. Mixing AS with UCSs dominated by electric fields

In Fig. 1 the energy evolution of some typical particles traveling inside a mixture of stochastic and systematic scatterers ($P = 0.5$) is shown. The synergy of stochastic acceleration by the AS (classical random walk like behavior) with systematic acceleration at the UCSs (sudden increases of energy) is apparent.

As described above, the particles travel and interact

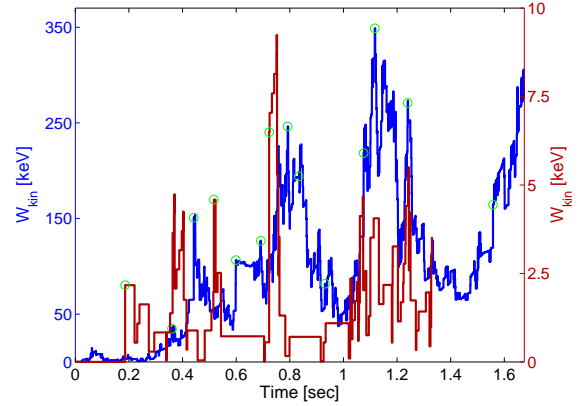


Figure 1. Kinetic energy of typical electrons as a function of time.

with scatterers until they exit the acceleration volume at some time, which is different for each particle. The median value of these times is the characteristic escape time (t_{esc}) for the ensemble, and it coincides with the half time $t_{1/2}$ of the system, defined as the time when half of the initial electron population has escaped. The energy distribution for the electrons that remain inside the volume exhibits a clear and extended power law tail for $P = 0$, with negligible heating at the low energies, but as P grows, the electrons are also heated under the influence of the magnetic disturbances, until they reach a combination of a hot plasma with a relatively small number of particles in the power law tail for $P = 0.5$, as shown in Fig. 2a.

The temperature of the heated low energy part of the distribution grows linearly with increasing P , starting from a value close to the initial temperature for $P = 0$, and reaching a much higher temperature of ≈ 130 keV for $P = 1$ (see Fig. 2b). On the other hand, the mean energy of the particles in the high energy tail increases with increasing P until it reaches a maximum value $\approx 17\text{--}18$ MeV, forming a plateau for the middle range of P values (0.3–0.7). For higher P values, the mean energy of the tail drops to ≈ 2 MeV. The synergy of the two classes of scatterers varies the behavior of the system from an efficient accelerator, when the UCSs dominate, to an efficient and excessive heating mechanism combined with acceleration, when both types of scatterers are involved. The power-law tail consists of a small percentage ($\sim 2\text{--}5\%$) of the total number of particles injected initially for almost all P values, with the exception of the pure UCS case, $P = 0$ ([Isliker et al. 2017a](#)), where the high energy particles are almost 15% of the total number of particles at $t = t_{\text{esc}}$.

For any combination of the two types of scatterers, the distribution of the high energy particles develops a power law shape, which ultimately attains an asymptotic index k_{asym} . The time this occurs is a measure for

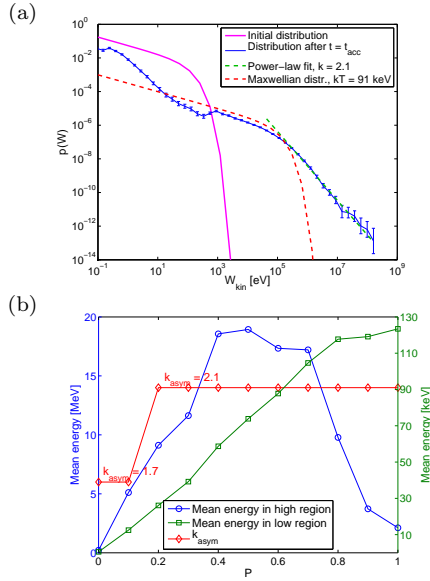


Figure 2. (a) Energy distribution of the electrons that stay inside until $t = t_{\text{acc}} \approx 1.7$ sec (blue), for $P = 0.5$; initial distribution (magenta); Maxwellian fit to the heated low energy region (red dashed), and fit to the power law tail (green dashed). (b) Mean energy at $t = t_{\text{esc}}$ for the high-energy tail (blue) and the heated low-energy region (green) for different ratios P of the two kinds of scatterers; the red points denote the asymptotic value k_{asym} of the power-law index.

the acceleration time of the system, t_{acc} . According to Fig. 2b, when the fraction of the ASs is low ($P < 0.2$), the index k_{asym} is 1.7, as in a pure UCS system, but as the influence of the ASs becomes stronger, we find $k_{\text{asym}} \approx 2.1$. The fraction of ASs also affects the acceleration time, which varies around 1.5–2 sec for $P \geq 0.2$, but it is much shorter for lower P values, e.g. ≈ 0.5 sec for $P = 0.1$ and a few milliseconds for $P = 0$. Electrons leave the system earlier when ASs are present. We can conclude from this parametric study of the energy distribution that the power law tail is a result of the synergy between the ASs and the UCSs, while the heating of the particles is a sole effect of the ASs.

2.3. The evolution of the escape time

As mentioned before, each particle exits the acceleration volume at a different time with a different energy. The escape time distribution adopts a power law shaped tail, as shown in Fig. 3a.

The distribution of the escape energy, i.e. the energy with which any particle escapes from the acceleration volume, exhibits the same behavior as the one of the particles that stay inside. The escape time and the escape energy depend on each other; the escape time as a function of the escape energy (determined through binned statistics) is shown in Fig. 3b for $P = 0.5$, compared also to the two “pure” cases ($P = 0$ and 1). We observe two distinct regions: For non-relativistic energies, 10^1 – 10^5 eV, a power law scaling is assumed, $t_{\text{esc}} \propto W_{\text{esc}}^{0.4}$.

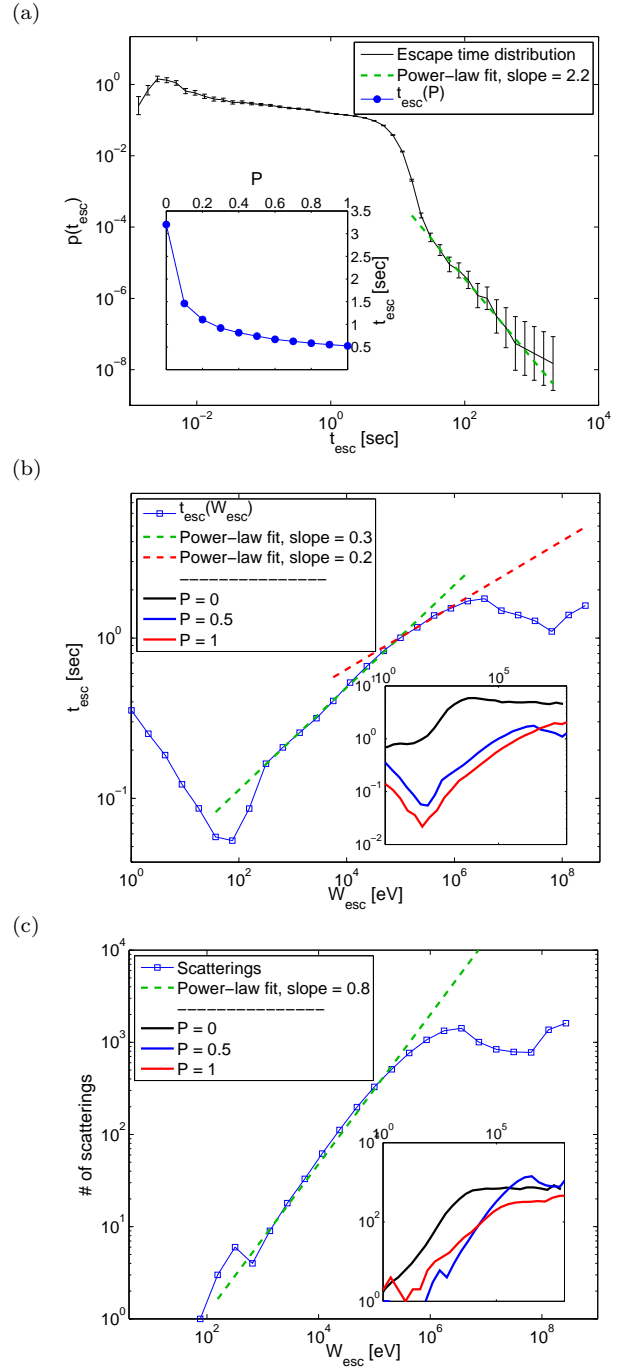


Figure 3. (a) Escape time distribution for $P = 0.5$; *inset*: the escape time distribution for different values of P . (b) The escape time as a function of the escape energy of the electrons for $P = 0.5$; *inset*: comparison between $P = 0$ (black), 0.5 (blue), and 1 (red). (c) Number of scatterings as a function of the escape energy of the electrons for $P = 0.5$; *inset*: comparison between $P = 0$ (black), 0.5 (blue), and 1 (red).

As for the relativistic energies, 10^5 – 10^9 eV, the functional form depends on P , e.g. for $P=0.5$ there is a power law scaling with index 0.2. In any case, the escape energy of the electrons is strongly related to the time the particles spend in the system, which is also

illustrated when considering the number of scatterings the escaping particles suffer before they escape from the simulation box as a function of their escape energy, see Fig. 3c (determined again through binned statistics), the escape energy increases with increasing number of scatterings, with a saturation at the highest energies.

All of the above results refer to electron populations. When ions are considered, no significant changes are observed. The energy distribution follows the same trends as in the electron case, with corresponding characteristics for the same values of P , similarly changing as P varies. Only the time scale is different, e.g. the escape time now extends from ≈ 130 sec for $P = 0$, to ≈ 5 sec for $P = 0.5$, and it reaches ≈ 3 sec for $P = 1$. UCSs are not only efficient accelerators, but they also keep the high energy plasma longer inside the simulation box.

3. DISCUSSION AND SUMMARY

In most explosive laboratory and astrophysical systems plasma heating is strongly correlated with particle acceleration. In the current literature the problems of heating and particle acceleration are studied separately. In explosive phenomena, particle acceleration has been related with reconnection, shocks, or weak turbulence, but no mechanism for the **impulsive heating** has been proposed so far (Lin et al. 2003).

In this article, we have shown that turbulent reconnection can be the solution to the combined problem, since the synergy of ASs and UCSs can provide both, the intense heating and the acceleration of the tail. The mixing of stochastic and systematic acceleration provides an asymptotic energy distribution that is heated substantially and exhibits a power law tail with index ~ 2 , which is close to the one estimated from the observations. The escape time of the particles depends on the fraction of the two types of scatterers and the energy of the particles. The lower the fraction of Alfvénic scatterers, the larger the escape time of the particles. The most energetic particles stay longest inside the acceleration volume (Krucker & Lin 2008). In the analysis presented in this article, we follow the evolution of

the energy distribution for **several seconds** in a **large scale open system**, where the magnetic disturbances and the UCSs have time to bring the energy distribution into an **asymptotic state**.

The scenario proposed here for most explosive phenomena in the solar atmosphere starts with the formation of large scale current sheets, which fragment very quickly, leading to turbulent reconnection. The UCSs impulsively (in a few milliseconds) accelerate the tail of the energy distribution, and soon after (a few seconds later) the ASs start participating by forming the super-hot sources and reinforcing the tail of the energy distribution (see a clear outline of the observations related to this scenario in Lin et al. 2003). The majority of the MHD simulations of explosive phenomena in the solar atmosphere rarely follow the fragmentation of the large scale current sheet, which is usually formed, nor do they consider the generation of magnetic disturbances, due to the limitations in the spatial resolution of these codes. Therefore, the formation of turbulent reconnection and its role in coronal heating and particle acceleration, as analyzed here, has so far been ignored.

The spatial transport inside a turbulent plasma will also influence the distribution of the accelerated particles (Bian et al. 2017), and the coupling of energy and spatial transport in turbulent reconnecting plasmas remains an open problem. The prompt acceleration and the impulsive heating by turbulent reconnection inside a large scale flaring magnetic topology and the anomalous transport in space will place the simple deterministic scenario for the interpretation of the Hard X-rays during solar flares, as proposed by (Brown 1971) almost 45 years ago and named “thick target model”, in a new frame of analysis. We claim that turbulent reconnection will provide answers to many open questions, possibly caused by the simplicity of the physical process adopted in the thick target model.

This work was supported by the national Programme for the Controlled Thermonuclear Fusion, Hellenic Republic. The sponsors do not bear any responsibility for the content of this work.

REFERENCES

- Ambrosiano, J., Matthaeus, W. H., Goldstein, M. L., & Plante, D. 1988, *Journal of Geophysical Research: Space Physics*, 93, 14383
- Arzner, K., Knaepen, B., Carati, D., Denewet, N., & Vlahos, L. 2006, *Astrophys. J.*, 637, 322
- Bian, N. H., Emslie, A. G., & Kontar, E. P. 2017, *ApJ*, 835, 262
- Biskamp, D., & Welter, H. 1989, *Physics of Fluids B*, 1, 1964
- Brown, J. C. 1971, *SoPh*, 18, 489
- Brunetti, G., & Lazarian, A. 2016, *MNRAS*, 458, 2584
- Burgess, D., Gingell, P. W., & Matteini, L. 2016, *Astrophys. J.*, 822, 38
- Cargill, P., Vlahos, L., Baumann, G., Drake, J., & Nordlund, Å. 2012, *Space science reviews*, 173, 223
- Cassak, P. A., & Drake, J. F. 2009, *ApJL*, 707, L158
- Chasapis, A., Retinò, A., Sahraoui, F., et al. 2015, *ApJL*, 804, L1
- Dahlin, J. T., Drake, J. F., & Swisdak, M. 2015, *Physics of Plasmas*, 22, 100704
- Dmitruk, P., Matthaeus, W., Seenu, N., & Brown, M. R. 2003, *The Astrophysical Journal Letters*, 597, L81

- Dmitruk, P., Matthaeus, W. H., & Seenu, N. 2004, *Astrophys. J.*, 617, 667
- Einaudi, G., & Velli, M. 1994, *Space Sci. Rev.*, 68, 97
- Fermi, E. 1949, *Physical Review*, 75, 1169
- . 1954, *ApJ*, 119, 1
- Galsgaard, K., & Nordlund, Å. 1996, *Journal Geoph. Res.*, 101, 13445
- . 1997a, *Journal Geoph. Res.*, 102, 219
- . 1997b, *Journal Geoph. Res.*, 102, 231
- Georgoulis, M. K., Velli, M., & Einaudi, G. 1998, *Astrophys. J.*, 497, 957
- Giannios, D. 2010, *MNRAS*, 408, L46
- Greco, A., Perri, S., & Zimbardo, G. 2010, *Journal of Geophysical Research (Space Physics)*, 115, A02203
- Guo, F., Liu, Y.-H., Daughton, W., & Li, H. 2015, *ApJ*, 806, 167
- Hoshino, M. 2012, *Physical Review Letters*, 108, 135003
- Hoshino, M., & Lyubarsky, Y. 2012, *SSRv*, 173, 521
- Islaker, H., Pisokas, T., Vlahos, L., & Anastasiadis, A. 2017a, *ArXiv e-prints*, arXiv:1709.08269
- Islaker, H., Vlahos, L., & Constantinescu, D. 2017b, *Physical Review Letters*, 119, 045101
- Karimabadi, H., Roytershteyn, V., Daughton, W., & Liu, Y.-H. 2013, *Space Science Reviews*, 178, 307
- Karimabadi, H., Roytershteyn, V., Wan, M., et al. 2013, *Physics of Plasmas*, 20, 012303
- Kontar, E. P., Perez, J. E., Harra, L. K., et al. 2017, *Physical Review Letters*, 118, 155101
- Kowal, G., de Gouveia Dal Pino, E. M., & Lazarian, A. 2011, *ApJ*, 735, 102
- Kowal, G., Falceta-Gonçalves, D. A., Lazarian, A., & Vishniac, E. T. 2017, *ApJ*, 838, 91
- Krucker, S., & Lin, R. P. 2008, *ApJ*, 673, 1181
- Kuramitsu, Y., & Hada, T. 2000, *Geophys. Res. Lett.*, 27, 629
- Lazarian, A., Eyink, G., Vishniac, E., & Kowal, G. 2015, *Philosophical Transactions of the Royal Society of London Series A*, 373, 20140144
- Lazarian, A., & Vishniac, E. T. 1999, *Astrophys. J.*, 517, 700
- Lazarian, A., Vlahos, L., Kowal, G., et al. 2012, *Space science reviews*, 173, 557
- Liang, J., Lin, Y., Johnson, J. R., Wang, X., & Wang, Z.-X. 2016, *Journal of Geophysical Research (Space Physics)*, 121, 6526
- Lin, R. P., Krucker, S., Hurford, G. J., et al. 2003, *ApJL*, 595, L69
- Loureiro, N. F., Uzdensky, D. A., Schekochihin, A. A., Cowley, S. C., & Yousef, T. A. 2009, *MNRAS*, 399, L146
- Malapaka, S. K., & Müller, W.-C. 2013, *ApJ*, 778, 21
- Matsumoto, Y., Amano, T., Kato, T. N., & Hoshino, M. 2015, *Science*, 347, 974
- Matthaeus, W. H., & Lamkin, S. L. 1986, *Physics of Fluids*, 29, 2513
- Matthaeus, W. H., & Velli, M. 2011, *Space Science Reviews*, 160, 145
- Onofri, M., Islaker, H., & Vlahos, L. 2006, *Physical Review Letters*, 96, 151102
- Onofri, M., Primavera, L., Malara, F., & Veltri, P. 2004, *Physics of Plasmas*, 11, 4837
- Osman, K. T., Matthaeus, W. H., Gosling, J. T., et al. 2014, *Physical Review Letters*, 112, 215002
- Parker, E. N. 1983, *Astrophys. J.*, 264, 635
- . 1988, *Astrophys. J.*, 330, 474
- Pisokas, T., Vlahos, L., Islaker, H., Tsiolis, V., & Anastasiadis, A. 2017, *ApJ*, 835, 214
- Rappazzo, A. F., Velli, M., & Einaudi, G. 2010, *Astroph. J.*, 722, 65
- . 2013, *Astroph. J.*, 771, 76
- Sironi, L., Petropoulou, M., & Giannios, D. 2015, *MNRAS*, 450, 183
- Turkmani, R., Vlahos, L., Galsgaard, K., Cargill, P., & Islaker, H. 2005, *The Astrophysical Journal Letters*, 620, L59
- Uritsky, V. M., Roberts, M. A., DeVore, C. R., & Karpen, J. T. 2017, *ApJ*, 837, 123
- Vlahos, L., Pisokas, T., Islaker, H., Tsiolis, V., & Anastasiadis, A. 2016, *Astrophys. J.*, 827, L3
- Wang, L. C., Li, L. J., Ma, Z. W., Zhang, X., & Lee, L. C. 2015, *Physics Letters A*, 379, 2068
- Zank, G. P., Hunana, P., Mostafavi, P., et al. 2015, *ApJ*, 814, 137